https://doi.org/10.2352/ISSN.2470-1173.2017.17.COIMG-439

Non-iterative joint demosaicing and super-resolution framework

X. Petrova, I. Glazistov, S. Zavalishin, V. Kurmanov, K. Lebedev, A. Molchanov, A. Shcherbinin, G.Milyukov, I. Kurilin; Samsung R.D. Institute Rus.; Moscow, Russia

Abstract

Inverse quadratic problem of joint demosaicing and multi-frame super-resolution(SR) was considered. Closed form solutions for different constant sub-pixel motions between frames were obtained and represented in the form of filter bank, which allows to compute solution of SR problem using adaptive filtering, where filters are selected depending on sub-pixel motion between frames. This procedure can be carried out using single iteration. For directional and non-directional parts of image corresponding directional or non-directional filters were applied. Color artifact reduction was achieved via usage of linear cross-channel regularizing term inspired by popular demosaicing methods. The framework includes motion estimation in Bayer domain, integrated noise reduction sub-algorithm, directionality estimation sub-algorithm, fallback logics and post-processing for additional color artifact reduction. Bank of filters is computed offline using specially developed compression techniques, which allows to reduce number of actually stored filters. Developed solution had shown superior results, compared to subsequent demosaicing and single channel SR and was tested on real raw images captured by cell phone camera in burst mode.

Super-resolution problem

Super-resolution(SR) is the name of techniques that allows to construct single high resolution (HR) image out of several observed low resolution (LR) images (Fig. 1). Compared to single frame interpolation SR reconstruction is able to restore high frequency component of the HR image exploiting complementary information from multiple LR frames. SR problem can be stated as described in [1].

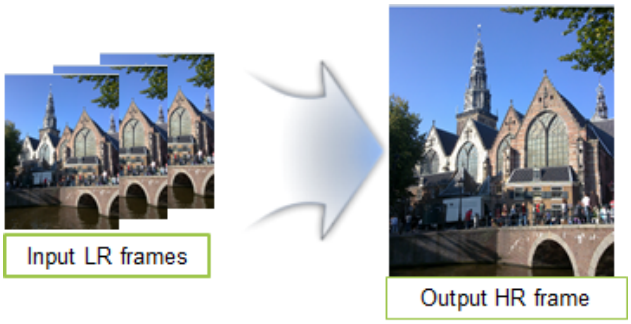

Figure 1. *Multi-frame SR*

Let X be the HR image that we are trying to reconstruct and Y_k be the k-th observation. The way each LR observation is obtained from HR image can be described by $Y_k = W_k \cdot X + V$, where W_k is image formation operator for k-th observation and V is noise term. Operator W_k can be composed out of warp M_k, blur G, decimation D, or other components, such as Bayer decimation B:

$$W_k = D \cdot G \cdot M_k \tag{1}$$

$$W_k = B \cdot D \cdot G \cdot M_k \tag{2}$$

In case, when image formation model includes Bayer decimation, the problem deals with joint demosaicing and SR. Thus, sought SR image X can be found out of the matrix equation

$$\mathbf{Y} = \mathbf{W} \cdot \mathbf{X} + V, \tag{3}$$

where $\mathbf{Y} = \begin{vmatrix} Y_1 \\ Y_2 \\ \dots \\ Y_n \end{vmatrix}$, $\mathbf{V} = \begin{vmatrix} V_1 \\ V_2 \\ \dots \\ V_n \end{vmatrix}$, $\mathbf{W} = \begin{vmatrix} W_1 \\ W_2 \\ \dots \\ W_n \end{vmatrix}$ and n is the number of LR images. As long as V is unknown and is assumed to be Gaussian noise, instead of solving problem 3, we can deal with optimization problem $\mathbf{X} = \text{argmin} \|\mathbf{W} \cdot \mathbf{X} - \mathbf{Y}\|^2$. In real life input data is insufficient for perfect reconstruction, so regularized problem

$$\mathbf{X} = \text{argmin}(\|\mathbf{W} \cdot \mathbf{X} - \mathbf{Y}\|^2 + \lambda \cdot \Gamma(\mathbf{X})), \tag{4}$$

is considered instead, where $\Gamma(\cdot)$ is regularization term.

Extensive reference to different types of norms, regularization terms and corresponding solvers used in different reconstruction frameworks (including SR, demosaicing, HDR imaging, etc.) can be found in [2]. Most of the research in SR is focused on the problem with quadratic data fidelity term and total variation(TV) regularization term. In case of non-linear and particularly non-convex form of regularization term the only way to find solution is iterative approach.

The goal of the present work was to obtain straightforward(without iterations) solution of joint SR and demosaicing problem, which can be used in consumer electronics devices like mobile phones or digital cameras.

Detailed explanation is provided below.

Filter bank representation of solution

We have chosen L_2 norm and quadratic regularization term $\Gamma(\mathbf{X}) = \lambda^2 \cdot (\mathbf{H} \cdot \mathbf{X})^T \cdot (\mathbf{H} \cdot \mathbf{X})$. In this case problem 4 is known to have closed form solution

$$\mathbf{X} = \mathbf{A} \cdot \mathbf{Y}, \mathbf{A} = (\mathbf{W}^T \mathbf{W} + \lambda^2 \cdot \mathbf{H}^T \mathbf{H})^{-1} \cdot \mathbf{W}^T.$$

It's important, that this solution depends on input data $\mathbf{Y}$ linearly. This means, that if we pre-compute set of matrices $\mathbf{A}$ for all possible shifts between LR frames and later use them for SR reconstruction (Fig. 2).

Although at the first sight this idea does not look meaningful, it will be shown, that after imposing a few additional constraints

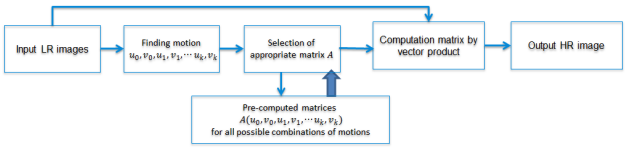

Figure 2. *General idea of pre-computing matrix* $\mathbf{A}$

it becomes possible to provide very compact representation of a set of matrices $\mathbf{A}$, sufficient for fairly accurate computation of SR problem solution. The way to obtain this compact representation is based on the following approaches:

- Reduce number of values to represent each matrix
  - ○Take in account matrix multilevel structure and use just a few lines from each matrix
  - ○Take in account banded structure to retain only a few elements from each line
- Reduce number of matrices needed to obtain reasonable accuracy
  - ○Use the same translational motion for every pixel of the image
  - ○Consider only sub-pixel motions
  - ○Use appropriate quantization of sub-pixel motions corresponding to accuracy of motion estimation procedure
  - ○Take in account symmetry properties of the problem

Let's describe additional constraints. The first constraint is related to regularization term, because all the further reasoning is highly dependent on it. We'll narrow our problem to particular choice of $\mathbf{H}$ in the form of 2D convolution operator with kernel $\hat{H}$, where $\hat{H} = \begin{vmatrix} -1/8 & -1/8 & -1/8 \\ -1/8 & 1 & -1/8 \\ -1/8 & -1/8 & -1/8 \end{vmatrix}$. This choice of $\mathbf{H}$ provided visually pleasing results on real images. Detailed analysis of applicability of our results to other types of regularization term is the matter of further research.

The second constraint is related to operator W_k. We'll consider only uniform relative translations of input LR images, where each k-th LR image is shifted with respect to decimated HR image by $s \cdot u_k$ pixels horizontally and by $s \cdot v_k$ vertically, where s is decimation factor (we assume that the same factor was used for horizontal and vertical decimation). In this case $\mathbf{A}$ is a function of $2 \cdot k$ values: $\mathbf{A} = \mathbf{A}(u_0, v_0, u_1, v_1, \ldots, u_n, v_n)$. On one hand this constraint provides means for initial reduction of number of matrices, on the other hand it is the reason of special multilevel structure of $\mathbf{A}$.

Let's consider single channel SR only (without demosaicing). Analysis of joint demosaicing and SR is a little bit more complicated, but the main idea is quite the same.

Let $\mathbf{X}$ be vectorized single channel image. To obtain colored output image the same procedure should be applied to each color channel (R,G,B) of input LR images separately.

Our numeric experiments with boundary conditions have shown that it makes no big difference whether to use Toeplitz or circular boundary conditions when constructing matrices M_k and G. Maximum difference of elements of matrix $\mathbf{A}$, corresponding to central pixels of HR image constructed for different boundary conditions is no more than 0.5%. Thus, we have preferred to use circular boundary conditions, which are beneficial from computational point of view, while reconstruction result just negligibly differs from results for physically motivated Toeplitz conditions.

Matrix $\mathbf{A}$ has specific structure, and we have performed some analysis inspired by [6], but here only practical conclusions will be mentioned.

If we add the third constraint that s is integer, matrix $\mathbf{A}$ for single channel SR problem can be completely described by it's s^2 lines(basic set) that are used to compute adjacent pixels of HR image, belonging to the same block of size $s \times s$. If for some index i, j there is a line belonging to the basic set, than these values are enough to construct a line for any other index i_1, j_1 satisfying $i_1 \mod s = i \mod s \,\&\, j_1 \mod s = j \mod s$. If LR image's dimension is $m \times m$, $\mathbf{A}$ will be completely described by only $s^2 \cdot n \cdot m^2$ out of $(s \cdot m)^2 \cdot (n \cdot m^2)$ values.

In [9] decay properties of multi-band matrices were studied. We have conducted numeric experiments to evaluate these properties for our case. Let's consider matrix $\mathbf{A}$ constructed for some small absolute values of u_k and v_k. Map of elements of $\mathbf{A}$ with absolute value more than 10^{-3} for $n = 3$ is shown in Fig. 3. It can be seen that no more than 5% of matrix element have significant absolute values. Fig. 4 explains extraction of a single line of

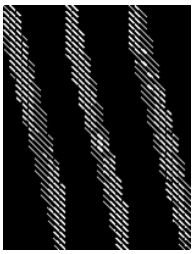

Figure 3. *Structure of matrix* $\mathbf{A}(n = 3)$.

matrix $\mathbf{A}$ corresponding to a single pixel of HR image, splitting this line into n parts, corresponding to LR images, and reshaping these parts to $m \times m$ matrices, where m is dimension of LR image. We can re-numerate elements of matrix $\mathbf{A}$ so that HR pixel

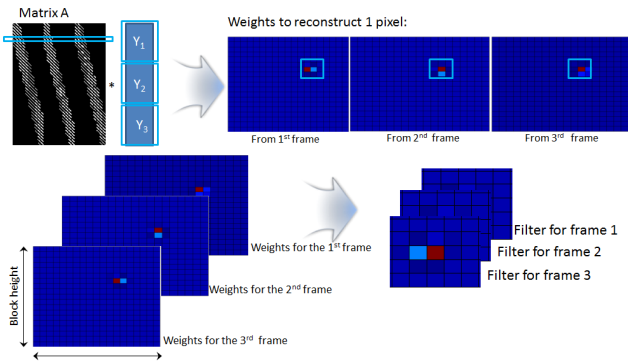

Figure 4. *Presenting* $\mathbf{A}$ *in filter form.*

with coordinates i, j will be computed as convolution of a certain vicinity of LR images in location $\frac{i}{s}, \frac{j}{s}$ with a 3D kernel

$$w(i \mod s, j \mod s, u_0, v_0, u_1, v_1, \ldots, u_n, v_n)$$

of some reasonable size

$$x_{i,j} = \sum_{k=0..n} \sum_{\hat{i}=-\varepsilon..\varepsilon} \sum_{\hat{j}=-\varepsilon..\varepsilon} w^k_{\hat{i},\hat{j}} \cdot y^k_{\frac{i}{s}+\hat{i},\frac{j}{s}+\hat{j}},$$

where $w^k_{\hat{i},\hat{j}} = a_{(i-1)\cdot m\cdot s+j,m^2\cdot(k-1)+(\frac{i}{s}+\hat{i}-1)\cdot m+\frac{j}{s}+\hat{j}}$ and notation $a_{\alpha,\beta}$ refers th the element of matrix $\mathbf{A}$ with corresponding coordinates. Let's consider value $P_\varepsilon = \frac{\sum_{k=0..n}\sum_{\hat{i}=-\varepsilon..\varepsilon}\sum_{\hat{j}=-\varepsilon..\varepsilon}|w^k_{i,j}|}{\sum_{\beta=1..m^2\cdot k}|a_{(i-1)\cdot m\cdot s+j,\beta}|}$. Fig. 4 shows, that this value becomes very close to 1 for quite small values of ε.

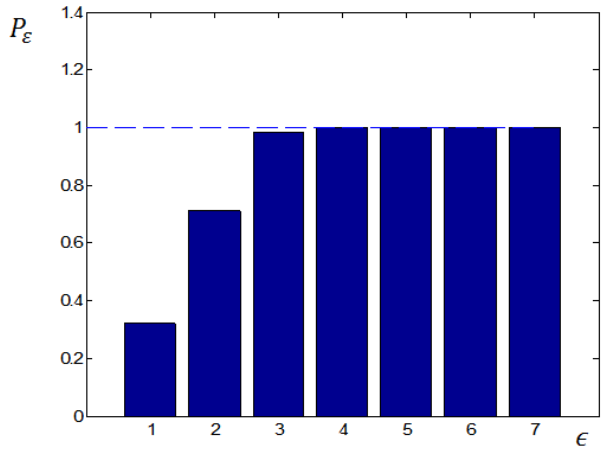

Figure 5. *Dependency of the proportion of energy of filter coefficients inside ε-vicinity of the central element from vicinity size*

This means than a single line of $\mathbf{A}$ can be accurately enough reconstructed from a 3D filter consisting of $n\cdot(2\cdot\varepsilon+1)^2$ values. The whole matrix can be reconstructed from $s\times s$ filters with dimensions $n\times(2\cdot\varepsilon+1)\times(2\cdot\varepsilon+1)$. Fig. 4 proves, that fo single channel SR assuming $|u_k|<1,|v_k|<1$ we can take $\varepsilon=5$ which means that filter w may have dimension $n\times 11\times 11$. Although assumption about small absolute values of $|u_k|$ and $|v_k|$ have direct impact on the value of ε, thanks to structure of $\mathbf{A}$ we can store only filters, computed for $|u_k|<1,|v_k|<1$. Suppose we need to solve SR problem for $\tilde{u}_0,\tilde{v}_0,\tilde{u}_1,\tilde{v}_1,\ldots,\tilde{u}_n,\tilde{v}_n,$, where some or all $|\tilde{u}_k|>1,|\tilde{v}_k|>1$. If we have a filter

$$w(i \mod s, j \mod s, u_0, v_0, u_1, v_1, \ldots, u_n, v_n),$$

where $u_k=\tilde{u}_k-round(\tilde{u}_k), v_k=\tilde{v}_k-round(\tilde{v}_k)$, HR pixel can be computed as

$$x_{i,j}=\sum_{k=0..n}\sum_{\hat{i}=-\varepsilon..\varepsilon}\sum_{\hat{j}=-\varepsilon..\varepsilon} w^k_{i,\hat{j}}\cdot y^k_{\frac{i}{s}+round(\tilde{u}_i)+\hat{i},\frac{j}{s}+round(\tilde{v}_k)+\hat{j}}, \quad (5)$$

Due to decay property only a few nearest corresponding LR pixels are used to reconstruct each HR pixel, which means that our initial assumption about uniform translational motion, which can hardly hold in practice for the whole image, should now hold only in ε vicinity of each pixel. Such assumption typically holds and this means that approach shown in Fig. 6 can be implemented in practice. Decay property also means that while using circular boundary conditions accurate filter values can be obtained from rather a small matrix $\mathbf{A}$. As matrix inversion has $O(n^3)$ complexity, this might have been a severe limitation otherwise. Let's conclude explanation above by a small numeric example. Suppose we have a 16×16 LR image, decimation factor $s=4$ and number of LR images $n=3$. If we tried to store the whole matrix $\mathbf{A}$ it would have been necessary to memorize $(16\cdot 4)\cdot(16\cdot 4)\times(16\cdot 16\cdot 3)=3,145,728$ values. In compact form it's possible to store only $(4\cdot 4)\times(3\cdot 11\cdot 11)=5,808$ values, which is 0.18% of the original number. Since filters are already computed, computing one pixel of HR image requires $n\cdot(2\cdot\varepsilon+1)^2$ multiplications (in the example above this will be 363) and $n\cdot(2\cdot\varepsilon+1)^2-1$ additions (disregarding complexity of motion estimation and other sub-algorithms).

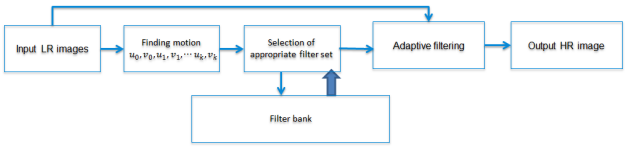

Figure 6. *SR with representation of pre-computed matrix A in the form of filter bank*

Let's consider more facts, that allow to reduce the number of considered $\mathbf{A}'\mathbf{s}$. If rounding operation means rounding towards nearest integer, we can pre-compute filters only for

$$-1/2\le u_k<1/2,-1/2\le v_k<1/2.$$

We also can assume that $u_0=v_0=0$ so matrix $\mathbf{A}$ is a function of only $2n$ parameters.

Since in practice motion estimation is done with some limited accuracy (we can consider $1/4$ pixel accuracy as a reasonable estimate) quite a few quantization levels of shifts should be considered. For q quantization levels of for sub-pixel motions and $n+1$ input observations (0^{th} observation with zero shift) only q^{2n} possible $\mathbf{A}'\mathbf{s}$ should be considered. For 4 quantization levels $(-1/2,-1/4,0,1/4)$, 3 input LR images ($n=2$) and $s=4$ all possible solutions will be described by 256 sets of 16 filters with dimensions $3\times 11\times 11$. These pre-computed values can be stored in the filter bank and appropriate filters can be selected based on value of sub-pixel motion, as shown in Fig. 7. Here block "core SR algorithm" implements expression 5 for each pixel.

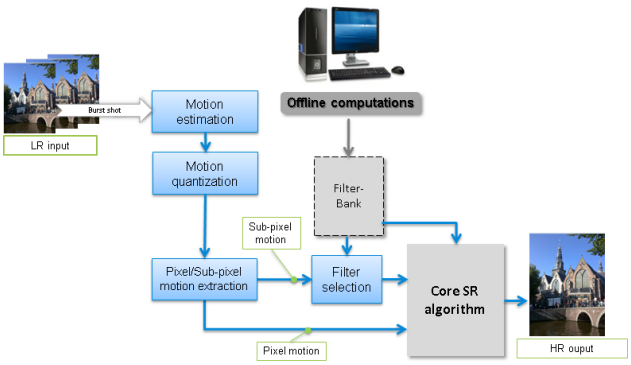

Figure 7. *Single channel SR algorithm outline*

In section some prospects of reducing number of stored values and complexity of obtaining single operator $\mathbf{A}$ are covered.

Joint demosaicing and super-resolution

Approach described in the section above can be used for the problem of joint demosaicing and SR. The difference would be in

using 2 instead of 1. In this case unknown vector will be formed out of stacked color channels $\mathbf{X} = \begin{vmatrix} X_R \\ X_G \\ X_B \end{vmatrix}$.

In this case we had to modify regularization term to introduce cross-channel regularization. Unlike [3] we've used a linear term:

$$\tilde{\mathbf{H}} = \begin{vmatrix} \mathbf{H} & 0 & 0 \\ 0 & \mathbf{H} & 0 \\ 0 & 0 & \mathbf{H} \\ \mathbf{H_c} & -\mathbf{H_c} & 0 \\ \mathbf{H_c} & 0 & -\mathbf{H_c} \\ 0 & \mathbf{H_c} & -\mathbf{H_c} \end{vmatrix}. \quad (6)$$

We have taken $\mathbf{H_c} = \gamma \cdot \mathbf{H}, \gamma = 3$. Compared to single channel solution described in section , sub-pixel shifts should be considered in the interval $[0,2)$ and 3 sets of filters, corresponding to color channels, should be stored. Fig. 8 shows, that joint demosaicing and SR performs better, than demosaicing followed by single channel resolution. Some more comparison results, including our

Figure 8. *(left) [5] demosaic + RGB SR (right) Bayer SR*

implementation of joint demosaicing and SR approach, described in [2] with cross-channel regularization term, described in [3] are provided in 9. It can be seen, that using a simple linear regularization term can be sufficient to obtain reasonable quality.

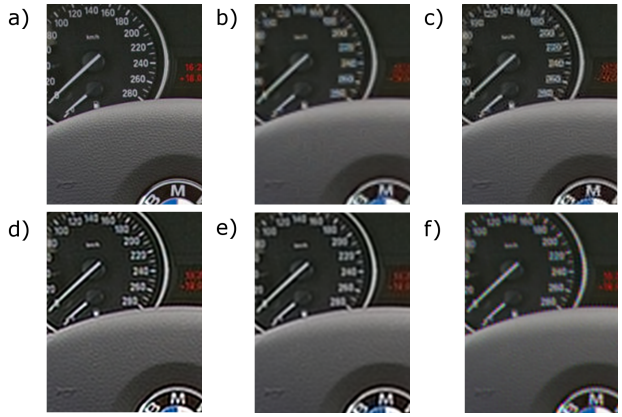

Figure 9. *Sample results of joint demosaicing and SR on rendered sample with known translational motion (a) ground truth; (b) demosaicing from [4]+bicubic interpolation; (c) demosaicing from [4]+ RGB SR (d) Bayer SR, smaller regularization term; (e) Bayer SR, bigger regularization term; (f) Our implementation of bayer SR from [2] with cross-channel regularization term from [3]*

Numeric evaluation on synthetic samples

We have performed numeric evaluation of SR algorithm quality on synthetic images in order to concentrate on core algorithm performance without considering issues of accuracy of motion estimation. We have used an image on Fig. 10, which contains several areas which are typically challenging for demosaicing algorithms.

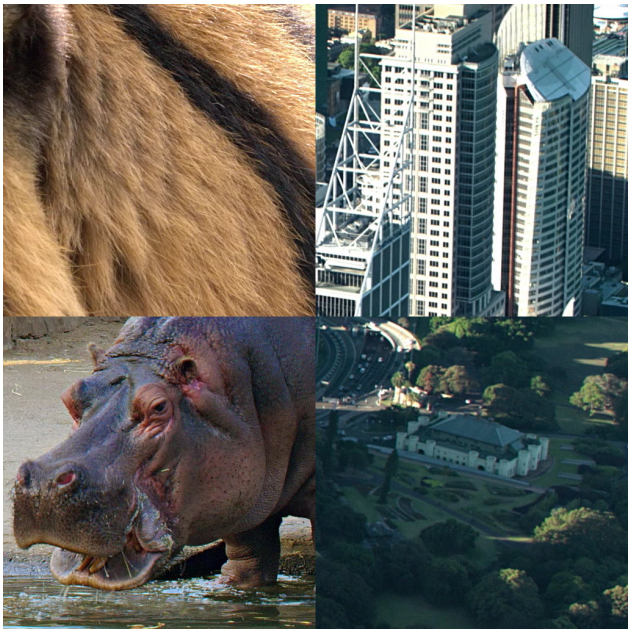

Figure 10. *Test image*

As far as reconstruction quality depends on displacement between low resolution frames (worst corner case: all the images are exactly the same), we have conducted statistical experiment with randomly generated motions Fig. 10. No wonder, that results for green channel, which is sampled more densely, results are better than in blue and red channels, where quality is quite the same. Fig. 11 explains influence of number of LR frames and multiplier *lambda* at the regularization term on restoration PSNR. This figure makes clear the following facts:

- Different sub-pixel shifts provide differrent PSNR for the same image, which means that for accurate evaluation of SR setup many possible combinations should be checked
- It's possible to find globally optimal multiplier *lambda*
- Increasing number of LR frames leads to higher PSNR, so number of frames is limited only by shooting speed and solution complexity
- Green channel can be reconstructed with higher accuracy than red and blue channel

As it was expected, this chart helps to make the best choise of ; increasing number of LR frames leads to increasing opfg Table 1 shows median values of PSNR obtained for different experimental settings (red channel). We have tested cases with 2,3 and 4 input frames and single channel and joint demosaicing and SR (Bayer SR) configurations. As far as number of stored filters increases dramatically while increasing magnification ratio, we also compares true 4X SR and 2X SR with subsequent 2X bicubic upscaling. For 4 input frames and Bayer SR we have obtained more than 3dB enhancement in average.

To check potential of reducing computational load by filter truncation, we have also checked PSNR in case of truncated ker-

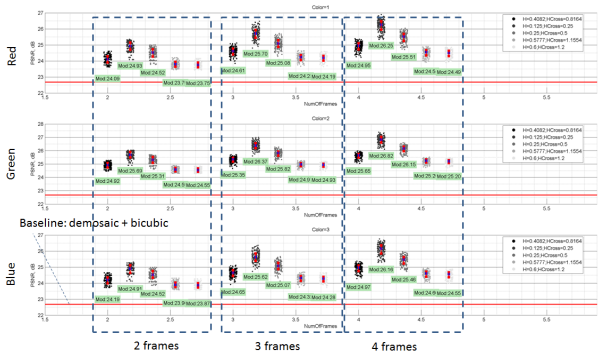

Figure 11. *Evaluation results on synthetic test*

Simulation results on synthetic samples (4X magnification, red channel)

MV Rounding	Domain	Demosaicing method	Config.	2 Frames	3 Frames	4 Frames
No	RGB	[5]	4X↑SR	23.5	23.7	23.9
Yes				23.4	23.6	23.7
No		[4]		24.3	24.5	24.6
Yes				24.0	24.3	26.3
No	Bayer	N/A	2X↑SR+2X↑	24.6	25.2	25.6
Yes				23.3	23.4	23.5
No			4X↑SR	**24.9**	**25.7**	**26.3**
Yes				24.5	25.2	25.6
No	RGB	[5]	2X↑SR+2X↑	23.5	23.7	23.9
Yes				22.8	22.9	23.0
No		[4]		24.1	24.2	24.5
Yes				23.4	23.5	23.5
N/A	RGB	[5]	4X↑	23.0		

nel. Table 2 shows, that filter size can be safely decreased to 12×12. Further truncation caused significant PSNR drop. In this set up we have also checked, if 2X SR is the same as X4 SR with subsequent downscaling. Untill now we haven't figured out how to modify 2X SR problem posing to obtain exactly the same results as 4X SR. It can be seen that X4+downscaling can provide in average more than 4dB gain.

Influence of kernel size (Bayer, 2X magnification, red channel)

Kernel size	Zoom config.	2 Frames	3 Frames	4 Frames
16×16	4X↑ SR + 2X↓ Bicubic	30.93	31.75	32.12
	2X↑ SR	29.34	30.19	30.25
14×14	4X↑ SR + 2X↓ Bicubic	30.93	31.75	32.12
	2X↑ SR	29.34	30.04	30.26
12×12	4X↑ SR + 2X↓ Bicubic	30.93	31.72	32.12
	2X↑ SR	29.33	30.05	30.25
N/A	[4] demosaicing + 2X↑ Bicubic	27.95		

Filter bank compression and fast filter bank computation

Taking in account symmetry inherent to solution of SR problem, it is possible to reduce significantly number of stored values (volume) needed to describe closed form solutions of SR problem. For example, for joint demosaicing and SR solution ($n = 3, s = 2$) solution volume was decreased for about 80 times, and for single channel SR ($n = 3, s = 4$) more than 40 times. We suppose to prepare a separate with proofs and detailed description of such compression technology. Besides, taking account special types of matrices involved in computation, advanced methods for block circulant matrices can be used. Thus, for size of high resolution block $n \times n$ solution requires $O(n^2 \log n)$ instead of $O(n^6)$ operations needed for matrix inversion. This work will be also described in other paper.

Integrated solution

For application in real life conditions we have implemented integrated solution, containing some additional sub-algorithms and features (Fig. 12), such as motion estimation in bayer domain, fallback logics, integrated noise reduction and some more additional features. We have found, that our Bayer SR algorithm

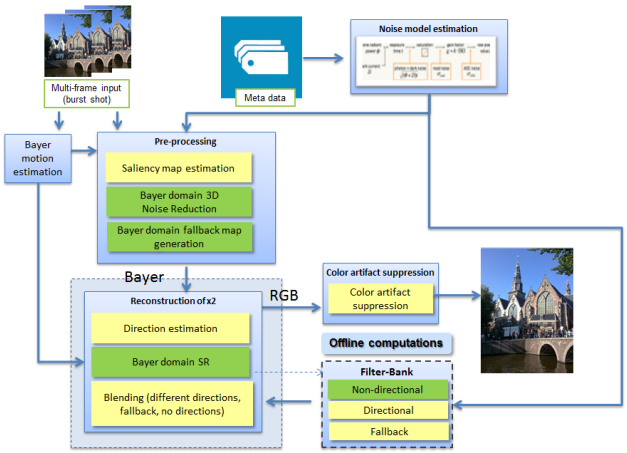

Figure 12. *Algorithm structure*

for some motions performs poorly on edges, and developed edge directional reconstruction filters to applied for strongly directional areas (Fig. 13). Fig. 14 shows sample output of directional mask

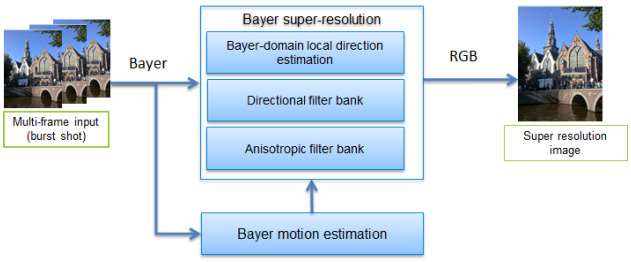

Figure 13. *Structure of directionality adaptation sub-algorithm*

estimation (marked by color) and Fig. 15 shows difference between directional and non-directional processing. Still, it is crucial not to use directional adaptation in non-directional areas, like shown in Fig. 18, where anisotropic filters descriobed in section were applied. In order to control noise reduction and regularization term depending on noise level and saliency map, we have developed adaptation scheme shown in Fig. 16, which allows to obtain at the same time better detail level in textured areas and higher noise suppresion in flat areas (Fig. 17).

Some sample output for real images (burst shot in Bayer, 3 frames) is shown in Fig. 18.

Conclusion and future work

We have developed high quality multi-frame joint demosaicing and SR (Bayer SR) solution which does not use iterations and has linear complexity. Set of supplementary sub-algorithms was developed and integrated with core solution to obtain implementation robust to motion errors and fast motions, different noise levels

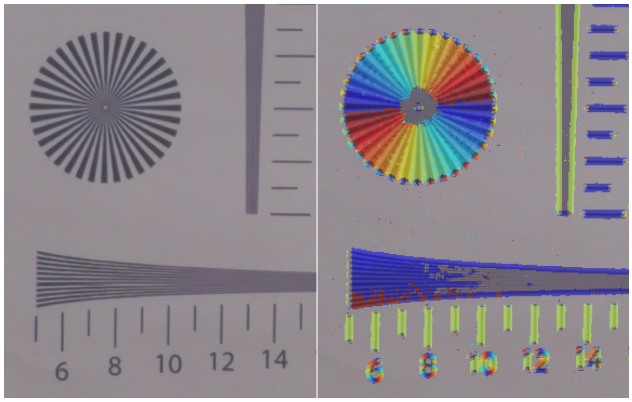

Figure 14. *(left) Input image (right) Directions marked by color wheel*

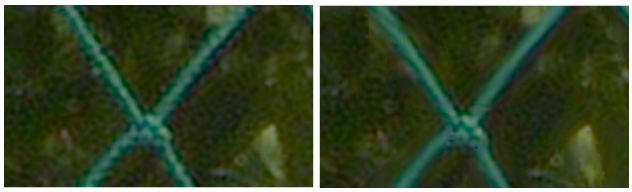

Figure 15. *(left) Without directionality adaptation, NR off (right) With directionality adaptation, NR off*

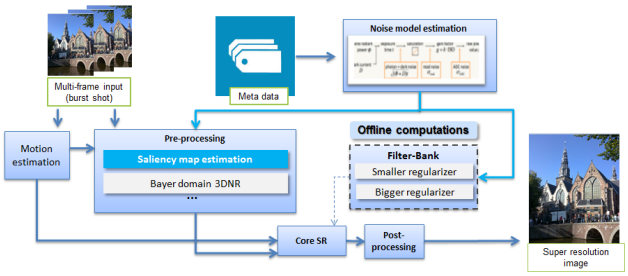

Figure 16. *Local salincy map-based NR power adaptation and choice of regularization term and NR power based on noise level*

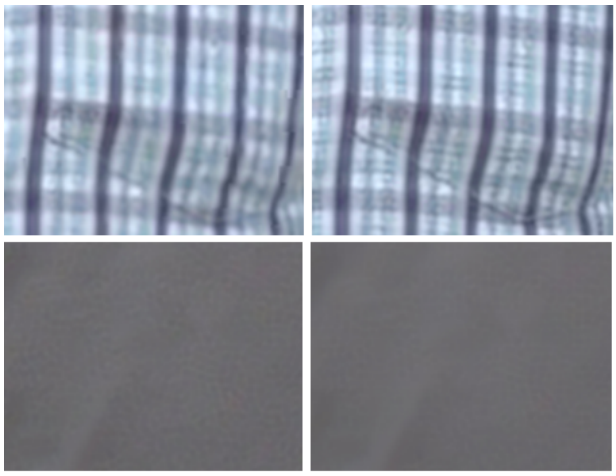

Figure 17. *(left) Salience-based adaptation off; (right) adaptation on*

and different textures. Our next step will be theoretical arrangement and parameter tunings along with providing clear theoretical description of methods, used for filter bank compression and fast computation of filters.

Figure 18. *Sample quality on real images. (top row) demosaicing from [4]+bicubic interpolation (bottom row) proposed*

References

[1] edited by Peyman Milanfar, Super-Resolution Imaging, IS&T, CRC Press (Taylor & Francis Group), 2010.

[2] Felix Heide, Markus Steinberger, Yun-Ta Tsai,Mushfiqur Rouf, Dawid Pajak, Dikpal Reddy, Orazio Gallo, Jing Liu, Wolfgang Heidrich, Karen Egiazarian, Jan Kautz, Kari Pulli, FlexISP: A Flexible Camera Image Processing Framework, ACM Transactions on Graphics (Proc. SIGGRAPH), vol. 33, N6, (2014).

[3] Felix Heide, Mushfiqur Rouf, Matthias B. Hullin, Bjorn Labitzke, Wolfgang Heidrich, Andreas Kolb, High-quality computational imaging through simple lenses, ACM Transactions on Graphics (TOG) TOG Homepage archive Vol. 32, 5, (2013), Article No. 149.

[4] Keigo Hirakawa, Thomas W. Parks, Adaptive homogeneity-directed demosaicing algorithm, IEEE Trans Image Process. 2005 Mar;14(3):360-9.

[5] Rico Malvar, Li-wei He, Ross Cutler, High-Quality Linear Interpolation for Demosaicing of Bayer-Patterned Color Images, ICASPP, Volume 34, Issue 11, pp. 2274-2282, (2004).

[6] Valentin V. Voevodin, Evgeny E. Tyrtyshnikov, Computational processes with Toeplitz matrices (in Russian), Physics and Mathematics literature pub. house "Science" (1987). https://books.google.ru/books?id=pf3uAAAAMAAJ

[7] Robinson, M. D., Toth, C. A., Lo, J. Y., and Farsiu, S. Efficient fourier-wavelet super-resolution. IEEE Transactions on Image Processing 19, 10 (Oct 2010), 2669-2681.

[8] Sroubek, F., Kamenick, J., and Milanfar, P. Superfast superresolution. In 2011 18th IEEE International Conference on Image Processing (Sept 2011), pp. 1153-1156.

[9] Mastronardi N., Ng M., Tyrtyshnikov E. E. Decay in Functions of Multiband Matrices, SIAM Journal on Matrix Analysis and Applications archive (July 2010) Volume 31 Issue 5, pp. 2721-2737

Author Biography

Xenya Y. Petrova received her MS in computer science (1998) and PhD(2002) in automatic control in St.-Petersburg University of Aerospace Instrumentation. Works in Samsung RnD Institute Russia since 2005 in the field of video and image processing(motion estimation, image enhancement, super resolution).

Ivan V. Glazistov received his MS degree in applied mathematics and computer science from Moscow State University (MSU), Russia in 2011. Since 2013 Mr. I. Glazistov has joined Image Processing Group, Samsung RnD Institute Russia where he is engaged in image and video processing projects.

Sergey S. Zavalishin received his MS degree in Computar Science from Moscow Engineering Physics Institute/University (MEPhI), Russia

in 2012. Currently he is a post graduate student of Ryazan State Radio Electronics University. His research interests include machine learning, computer vision and image processing.

Alexander A. Molchanov received his MS degree in applied mathematics and cybernetics from Moscow State University (MSU), Russia in 2012. Since 2012, A. Molchanov is a member of Image Processing Group at Samsung RnD Russia. His research interests include machine learning, computer vision and image processing.

Vladimir G. Kurmanov received his MS degree in Computer Science from Bauman Moscow State Technical University (BMSTU), Russia in 2014. In 2013, Mr. V. Kurmanov has joined Image Processing Group, Samsung RnD Institute Russia where he is engaged in image and video processing projects.

Kirill V. Lebdev received his MS degree in applied mathematics from Nizhny Novgorod State University (UNN), Russia in 1998. He has joined Samsung RnD Institute Russia in 2013 and joined to Image processing Group in 2016.

Gleb S. Milyukov received his specialist degree in applied mathematics from National Research Nuclear University MEPhI (Moscow Engineering Physics Institute), Russia in 2015. In Samsung RnD Institute Russia since 2013.

Ilya V. Kurilin received his MS degree in radio engineering from Novosibirsk State Technical University (NSTU), Russia in 1999 and his PhD degree in theoretical bases of informatics from NSTU in 2006.Since 2007, Dr. I. Kurilin has join Image Processing Group, Samsung RnD Institute Russia where he is engaged in photo and document image processing projects.